Supplemental Data. Noir et al. (2015). Plant Cell 10.1105/tpc.114.135301

Supplemental Figure 1. Diagram of the genomic locus of *FBL17* (modified from Gusti et al., 2009)
Dark grey represents the coding sequence whereas light grey indicates non-translated regions. The two T-DNA insertions corresponding to *fbl17*-1 and *fbl17*-2 mutants, respectively, are presented. The two black arrows (not to scale) give the localisation of the qPCR primers used to quantify *FBL17* transcript levels in Figure 2 A.

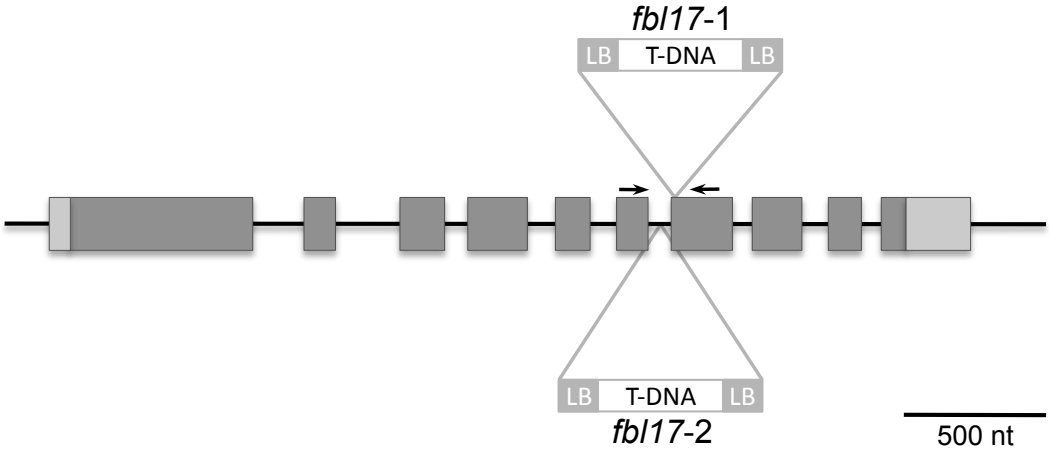

Supplemental Figure 2. *fbl17* null mutant plants are able to flower, but remained fully sterile.
(A) Fresh inflorescences of the indicated genotypes were collected to perform scanning electron microscopy observations of stigmas and anthers. Images were taken using the Tabletop Microscope TM-1000 (Hitachi).
(B) *FBL17* expression pattern using *pFBL17:GUS* promoter-reporter fusion lines. Representative picture of histochemical localization of GUS activity in flower. Scale bars are as indicated.

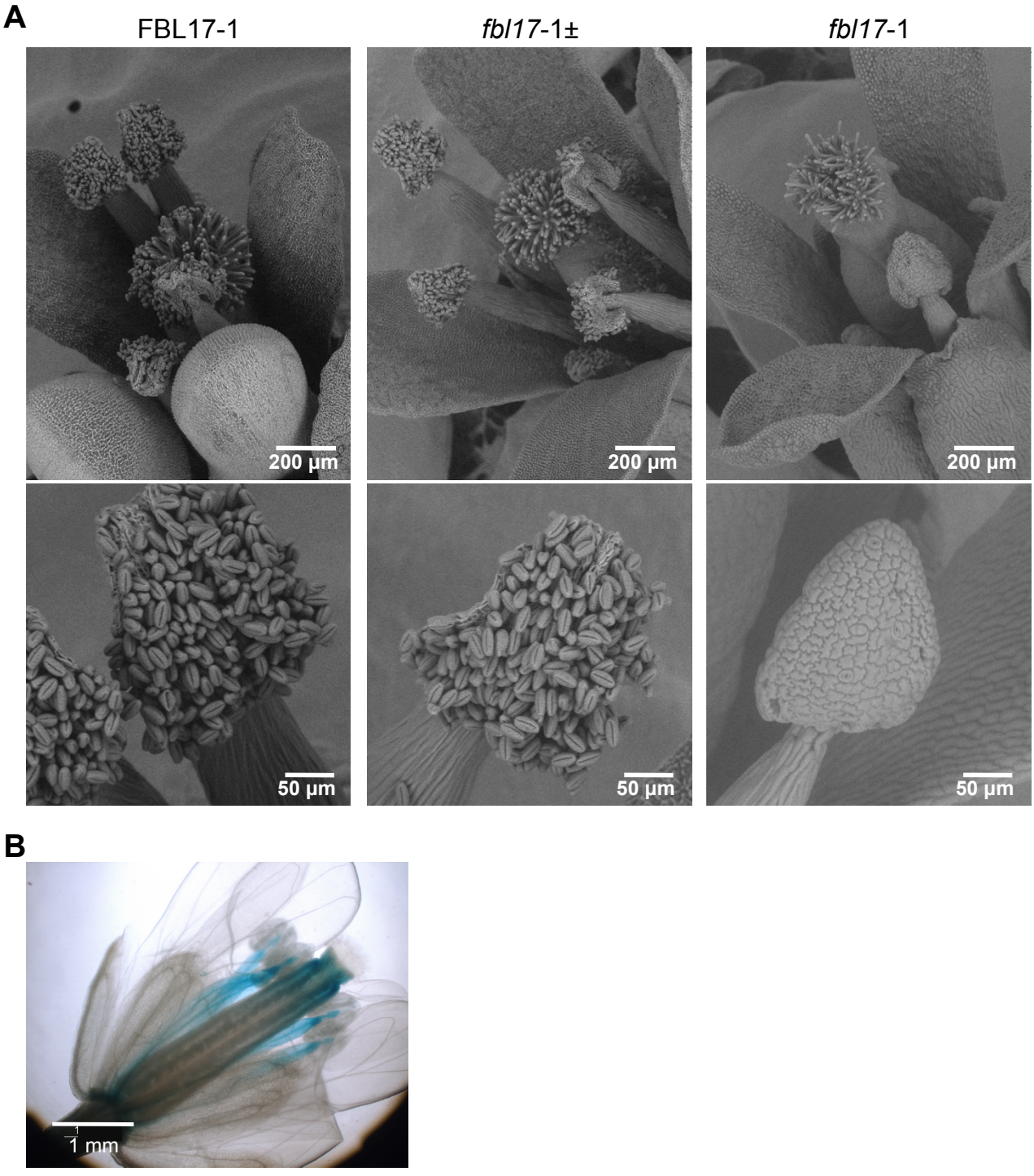

Supplemental Figure 3. Generation of transgenic *FBL17* knockdown lines using RNA interference.
(A) Schematic representation of the hairpin constructs used to generate transgenic *FBL17* knockdown lines by RNA interference (RNAi). The hairpin was expressed under the control of either the constitutive Cauliflower Mosaic Virus 35S promoter (35S:FBL17i lines) or the 868-bp *FBL17* endogenous promoter (pF17:FBL17i lines). **(B)** Relative expression levels of *FBL17* transcripts were determined by quantitative RT-PCR in first pair of leaves from 20-d-old seedlings of the indicated genotypes grown under *in vitro* conditions **(C)**. The bar graph depicts the expression level mean values of *FBL17* transcripts of a unique replicate (± standard errors of the technical triplicate). (**C**) Scale bars are 1 cm.

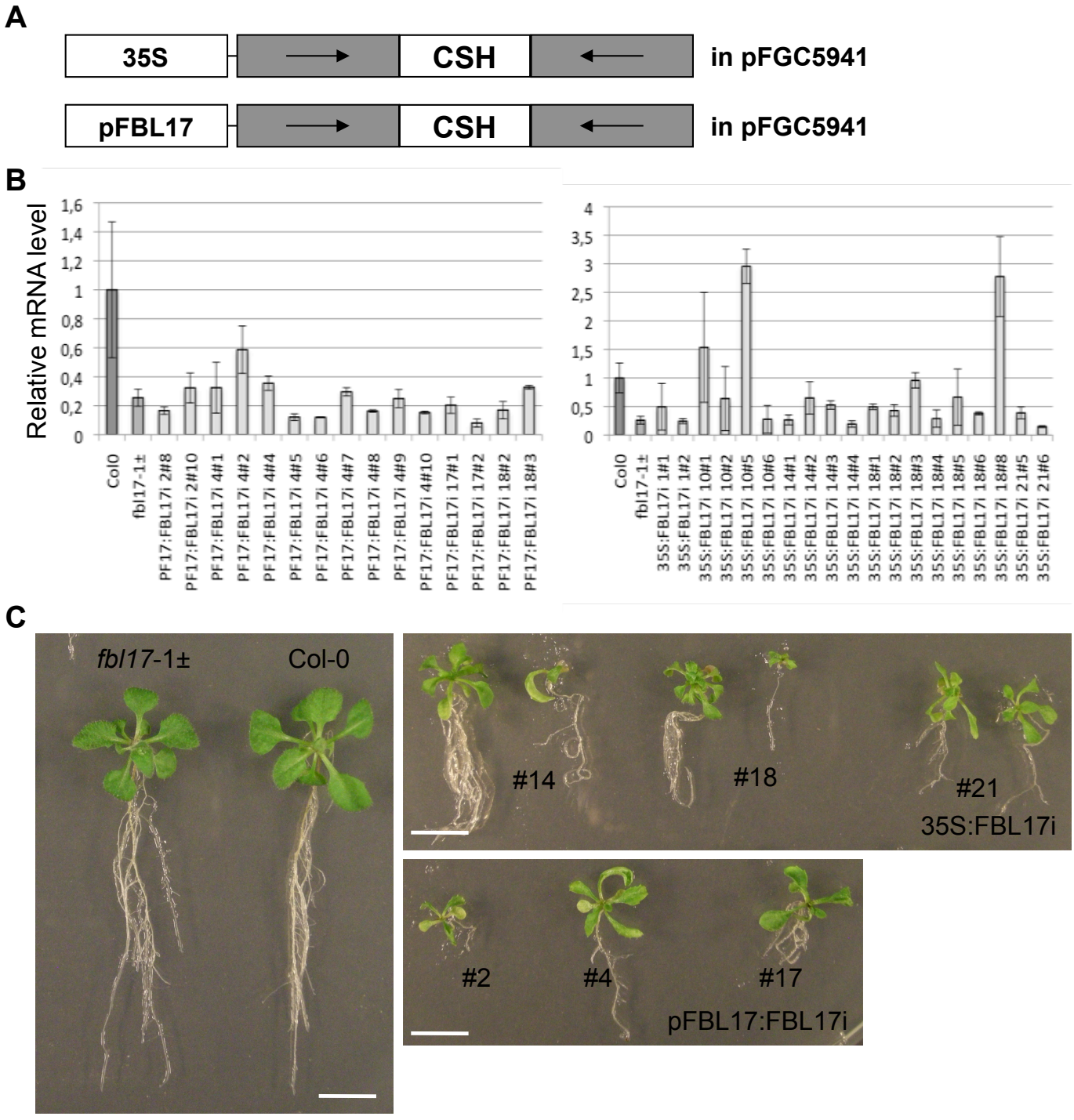

Supplemental Figure 4. *FBL17* loss of function results in supernumerary QC cells in root tip.
(**A**) Quantification of the number of cells exhibiting a GFP signal in the primary root tip of 10 d-old *pWOX5:GFP* transgenic lines grown under *in vitro* conditions. The values represent the average of two independent replicates. For each replicate, the analyses were performed on 9 and 7 *fbl17*-1 and, 9 and 6 wild-type (WT) root samples, respectively. Bars indicate standard deviations. (**B**) Expression pattern of the quiescent center (QC)-specific promoter trap line QC46 in wild type and *fbl17*-1 mutant background. Shown are light images of primary root tips of 10-d-old seedlings stained for 4 h; the lowest panel presents close-up pictures of the GUS-expressing cells of the above pictures, respectively. GUS signal in the wild-type root appears restricted to the QC cells, while GUS expression in the root tips of the *fbl17*-1 mutants extends to a broader number of cells. Scale bars are as indicated.

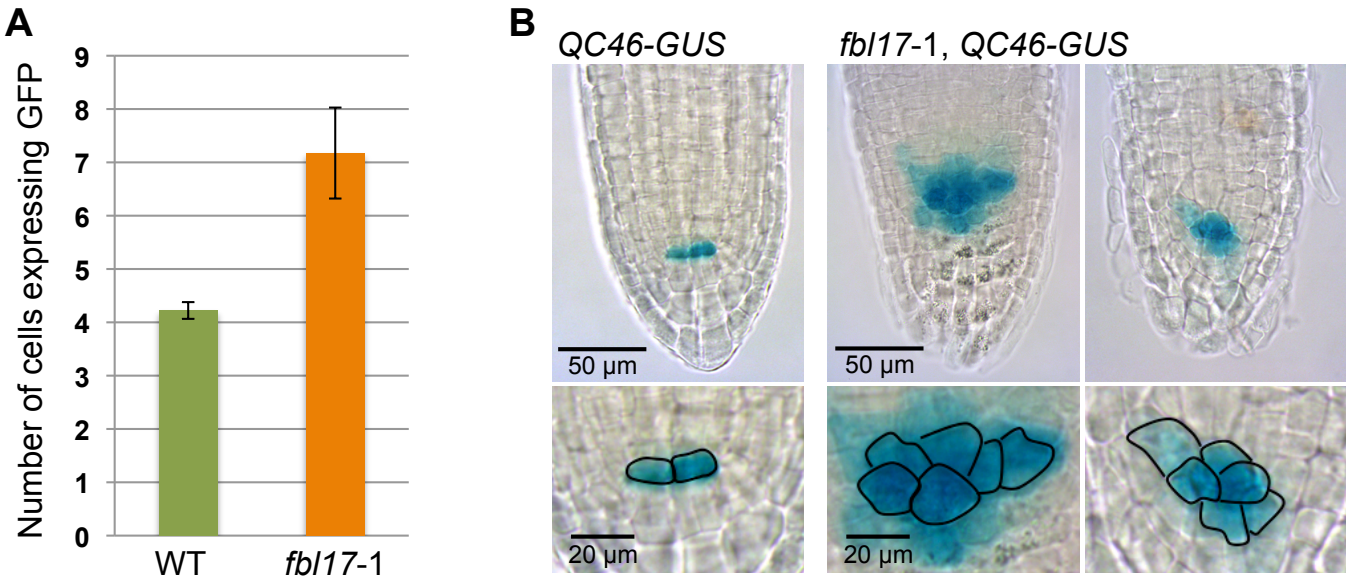

Supplemental Figure 5. *pCYCB1;1:Dbox-GUS* expression level is up-regulated in *FBL17* deficient lines. Histochemical GUS staining of wild-type and *fbl17*-1 null mutant seedlings expressing the *pCYCB1;1:Dbox-GUS* marker. The pictures show representative distribution pattern of GUS signals in 20-d-old seedlings grown under *in vitro* conditions after overnight GUS staining (left panels) and close-up pictures of primary root tips of 10-d-old seedlings after 1.5 h GUS staining (right panels). Scale bars are as indicated.

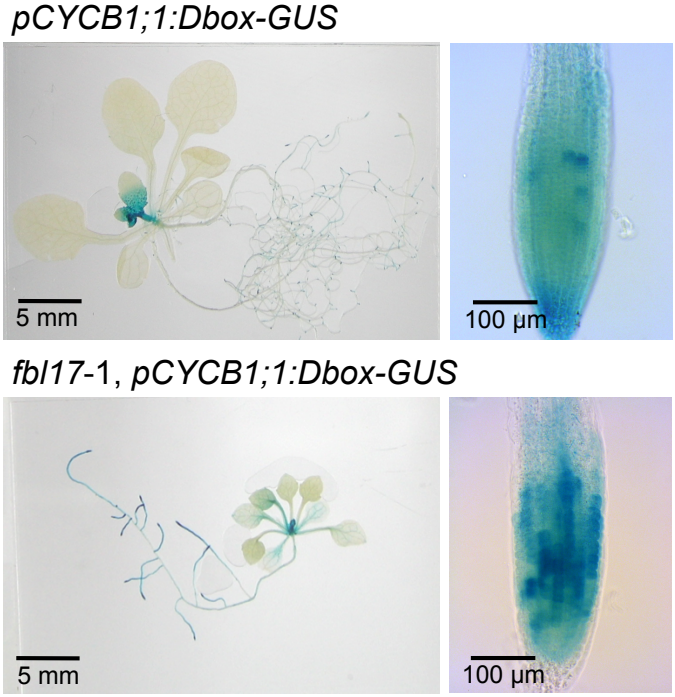

Supplemental Figure 6. *FBL17* loss-of-function root cells exhibit altered nucleus size and shape.
The box whisker graphs depict the bulked average data of 3 independent replicates. For each replicate, 23-24 and 6-17 nuclei were scored from wild-type and *fbl17*-1, HB2-YFP roots of 8-d-old *in vitro*-grown seedlings, respectively. Maximal (max. F, corresponding to the 'Feret' heading in ImageJ) and minimal (min. F, corresponding to the 'MinFeret' in ImageJ) Feret diameters represents respectively, the maximum and the minimum extension of the nucleus. The shape descriptor 'Circularity' gives an estimation of the roundness of the nucleus (a value of 1 indicates a perfect circle, and the closer the values to 0, the more elongated is the shape). Both maximal and minimal Feret parameters suggest a smaller size of the *fbl17*-1 nuclei while the circularity shape descriptor shows that mutant nuclei are less round than wild-type nuclei and also exhibit a wider distribution of shapes.

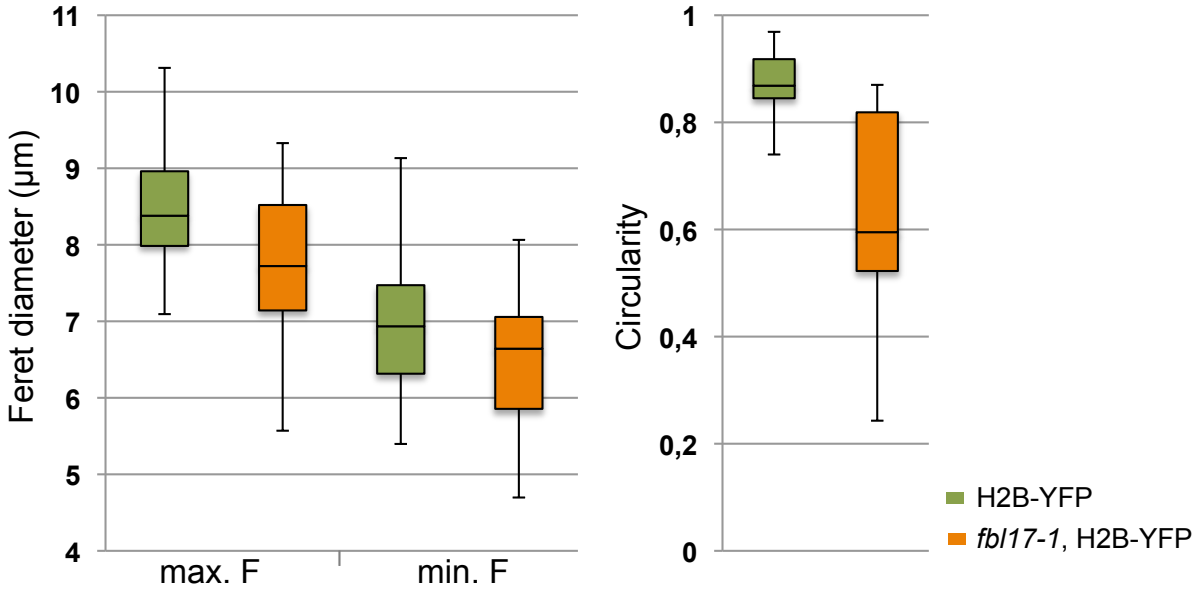

Supplemental Table 1. Frequency of homozygous *fbl17* mutants in the progeny of the indicated parental genotypes.

(**A**) *in vitro* culture

Parental genotype	**WT-like phenotype**	***fbl17* phenotype**	***fbl17* frequency (%)**
fbl17-1±	4851	59	1,22 [a]
fbl17-2±	3557	30	0,84 [b]

(**B**) culture on soil

Parental genotype	**WT-like phenotype**	***fbl17* phenotype**	***fbl17* frequency (%)**
fbl17-1±	9639	84	0,87 [c]
fbl17-1± *krp2*-3 *krp7*-1	5553	88	1,58 [d]
fbl17-1± *krp2*-1 *krp3*-1	6234	85	1,36 [d]
fbl17-1± *krp3*-2 *krp5*-1 *krp7*-1	7555	162	2,14 [c]

fbl17 frequencies are averages from [a]9, [b]4, [c]3, or [d]1 distinct progenies; WT=wild-type.

Supplemental Table 2. Primer combinations used for the genotyping of the T-DNA insertion lines.

T-DNA insertion line			5' -> 3' sequence
***fbl17*-1**	GABIkat_170E02	F	GAACTGCTTGATCTGAGTGGG
		R	CCAACTTCCTTCTCTTCCCTG
		T-DNA	CCCATTTGGACGTGAATGTAGA
***fbl17*-2**	GABIkat_436F11	F	GCCGAGAAGTTTTCAGAAACC
		R	TGTCAGTTTCCTTTTTATCCAGG
		T-DNA	CCCATTTGGACGTGAATGTAGA
***krp2*-1**	SALK_068815	F	TGCACTAATTGCACTGATTTTG
		R	AGACTCTTCCTTAACCTGCGG
		T-DNA	ATTTTGCCGATTTCGGAAC
***krp2*-3**	SALK_110338	F	TATTCCTTTACCACGTCAGCC
		R	GAGATTCTCCTCCGGTTGAAG
		T-DNA	ATTTTGCCGATTTCGGAAC
***krp3*-1**	GABIkat_185C07	F	CCCTCTTCGCTGATTGAACC
		R	CCTCTGTTGCTGCTGCTC
		T-DNA	CCCATTTGGACGTGAATGTAGA
***krp3*-2**	Wisc Ds-Lox 497-07H	F	TGCTATCTTCAGCTCCGTAGC
		R	TCAAACCAAAACCAAACATCC
		T-DNA	AACGTCCGCAATGTGTTATTAA
***krp5*-1**	SALK_053533	F	GATTCATCCGATGAGCAAATG
		R	GATTCATCCGATGAGCAAATG
		T-DNA	ATTTTGCCGATTTCGGAAC
***krp7*-1**	GABIkat_841D12	F	CGTTGAATTAATCAACGGCTC
		R	TCTTGGTACGAAGAACAGATGAAG
		T-DNA	CCCATTTGGACGTGAATGTAGA

Supplemental Table 3. Primer combinations used for cloning.

		5' -> 3' sequence
FBL17 promoter	F	GGGGACAAGTTTGTACAAAAAAGCAGGCTCCATCACCAAATC CTTGAG
	R	GGGGACCACTTTGTACAAGAAAGCTGGGTTCGTGAGATTTTG GGAG
FBL17 coding sequence	F	AAAAAGCAGGCTTAGAAGGAGATAGAACCATGCAACCTCAGC
	R	CGCATAGAAAGCTGGGTCATGTATAATGGTACACAT
FBL17 RNAi hairpin	F	XhoI-CTCGAGCAACCTCAGCCGCATATTTC
	R	NcoI-CCATGGCTCGATGTCTCTCTCCATCC
	F	SpeI-ACTAGTCAACCTCAGCCGCATATTTC
	R	XbaI-TCTAGACTCGATGTCTCTCTCCATCC
630-bp KRP2 fragment	F	CGGAATTCATGGCGGCGGTTAGG
	R	CCGCTCGAGTCATGGATTCAATTTAACC
6-HA fragment	F	CGCGTTTAAACCCGGGTCTAGATACC
	R	CGGAATTCAGATCTTCTAGAAGC

Supplemental Table 4. Primer combinations used for the quantitative RT-PCR analyses.

		5' -> 3' sequence
TIP4.1	F	GTGAAAACTGTTGGAGAGAAGCAA
At2g25810	R	TCAACTGGATACCCTTTCGCA
EXP	F	GAGCTGAAGTGGCTTCAATGAC
At4g26410	R	GGTCCGACATACCCATGATCC
FBL17	F	CTCGGGATGATCTGCGATGTC
AT3G54650	R	GACTTGGATTCTCTACAAAGGTCG
RBR1	F	TGAACTTTACGGCGCAGACT
AT3G12280	R	CGGAACCCACGTTTGTAGTATT
CDKB1;1	F	GCAATTGCTTCATATCTTCAGGTT
AT3G54180	R	CAGTCACGCAGTGTGGAAAC
CYCD3;1	F	CGAAGAATTCGTCAGGCTCT
AT4G34160	R	ACTTCCACAACCGGCATATC
CYCB1;1	F	CCCATATGGACCAGCACTCT
AT4G37490	R	CTTGTTGCTTCCATTGCTGA
CYCB1;2	F	CACACCGGCTACACAGAGTC
AT5G06150	R	GAAACCATAGCAACACCTCCA
BRCA1	F	CATGTGCCTTTTGTCAGTGTTCA
AT4G21070	R	AAATCCGCAGAGACAGGTTCA
E2FA	F	TGACGGATATTTGGAAAACTGACTC
AT2G36010	R	GGTGCTATTTCGCCCATTCC
ATR	F	TGCCATTCAGATTGACCCAGA
AT5G40820	R	CCCTCATGAAGATGCCCTCA
WEE1	F	CGTAAAGCTATGATGGAAGTGCAA
AT1G02970	R	GCTCATTTTCAAACCACGAGGA

Supplemental Methods

Plant Materials. The *FBL17* (At3g54650) T-DNA insertion lines *fbl17*-1 (Gabi-KAT_170-E02; Col-0 background), and *fbl17*-2 (Gabi-KAT_436-F11; Col-0 background), the *ICK2*/*KRP2* (At3g50630) T-DNA insertion lines *krp2*-1 (SALK_068815; Col-0 background; Moulinier Anzola et al., 2010), and *krp2*-3 (SALK_110338; Col-0 background; Sanz et al., 2011), the *ICK6*/*KRP3* (At5g48820) T-DNA insertion lines *ick6*-1/*krp3*-1 (Gabi-KAT_185-C07; Col-0 background; Moulinier Anzola et al., 2010; Cheng et al., 2013), and *krp3*-2 (Wisc Ds-LOX_497-07H), the *ICK3*/*KRP5* (At3g24810) T-DNA insertion line *krp5*-1 (SALK_053533; Col-0 background; Wen et al., 2013) and, the *ICK5*/*KRP7* (At1g49620) T-DNA insertion line *ick5*-1/*krp7*-1 (Gabi-KAT-841D12; Col-0 background; Moulinier Anzola et al., 2010; Cheng et al., 2013), were isolated and confirmed by PCR-based approaches. The *fbl17*-1± *krp2*-3 *krp7*-1, *fbl17*-1± *krp2*-1 *krp3*-1 and, *fbl17*-1± *krp3*-2 *krp5*-1 *krp7*-1 were generated by performing crosses and genotyping the resulting F_2 and/or F_3 progenies by PCR-based approaches. The Arabidopsis transgenic lines expressing *pCYCB1;1:Dbox-GUS* (Donnelly et al., 1999), the GUS-expressing promoter trap line QC46 (Sabatini et al., 1999), *pSCR:YFP* (Welch et al., 2007), *pSHR:SHR-GFP* (referred in the paper as *SHR-GFP*; Nakajima et al., 2001), *pWOX5:GFP* (Blilou et al., 2005), *H2B-YFP* (Dubin et al., 2008), *pTMM:GUS-GFP* (Nadeau and Sack, 2002) and the enhancer trap line E1728 (Gardner et al., 2009) were introgressed into the *fbl17* mutant background by crossing with the heterozygous *fbl17*-1±. In the resulting progenies, heterozygous *fbl17*-1± plants were distinguished from the wild-type (WT) plants using PCR-based genotyping (Table S2).

Generation of Arabidopsis transgenic lines. All primers used to generate the following described constructs are listed in Supplemental Table 3. Constructs were transformed *via* floral dip method as described by Clough et al. (1998) into Arabidopsis plants of Col-0 ecotype and into *fbl17*-1± heterozygous plants. The transgenic plants were selected for the appropriate resistance, and the presence of the corresponding transgene was verified. For each construct, 20-40 seedlings of six independent transgenic lines were tested at the T_2 generation

To generate the *pFBL17:GUS* construct, a *FBL17* native promoter sequence corresponding to the 868 base pairs of the 5´ upstream region of *FBL17* before the start-codon was amplified by PCR from genomic DNA of wild-type Col-0 Arabidopsis and cloned into the Gateway™ pDONOR221 vector (Invitrogen). After sequencing, this promoter sequence was

moved into the Gateway™ destination binary vector pGWB633 (Nakamura et al., 2010) by Gateway™ LR recombination reactions.

Transgenic *FBL17* knockdown lines were generated using RNA interference (RNAi). A 500-bp fragment in the first exon of *FBL17* (Supplemental Figure 2 and Supplemental Table 3) was cloned into the pFGC5941 vector (Kerschen et al., 2004) to generate a hairpin of *FBL17*. The hairpin was expressed under the control of either the constitutive Cauliflower Mosaic Virus 35S (35S) promoter (35S:F17i lines) or the 868-bp *FBL17* endogenous promoter, previously mentioned (pF17:F17i lines).

The coding sequence of *FBL17* was amplified by PCR from a cDNA sample of wild-type Col-0 ecotype Arabidopsis leaves and cloned into the Gateway™ pDONOR207 vector (Invitrogen). After sequencing, the *FBL17* fragment was moved into the Gateway™ destination binary vector pK7FWG2 (VIB, Gent, Belgium) by Gateway™ LR recombination reaction. The resulting construct, 35S:FBL17-GFP, allows the expression of FBL17 C-terminal-GFP fusion proteins under the control of the 35S promoter. This construct was further modified by excision of the 35S promotor using *Sal*I restriction enzyme and insertion of the 868-bp *FBL17* native promoter fragment. This construct is referred to as the *pFBL17:FBL17-GFP* binary construct.

Using a *KRP2* (At3g50630) cDNA clone as a template, a 630-bp *KRP2* fragment flanked by *EcoR*I and *Xho*I restriction sites, at 5' and 3' ends respectively, was amplified by PCR. A 6-HA fragment flanked by *Dra*I and *EcoR*I restriction sites, at 5' and 3' ends respectively, was also amplified by PCR from our vector collection. The two amplified fragments were agarose-gel purified and ligated into *Dra*I and *EcoR*I sites of the multiple cloning site of the Gateway™ pENTR-1A vector (Invitrogen). The resulting ENTRY clone, pENTR-6HA-KRP2, was sequenced to verify the absence of mutation, and then used to move the 6HA-KRP2 fragment into the destination binary vector pK7WGF2 (VIB, Gent, Belgium). The 35S:GFP-6HA-KRP2 construct generated is referred to as the *GFP-KRP2*^{OE} construct.

Nucleus size and shape estimation. Using the ImageJ 1.37 software (http://rsbweb.nih.gov/ij/), nucleus size and shape were estimated by scoring the maximal ('Feret' heading in ImageJ) and minimal ('MinFeret' heading) Feret diameters (*aka* caliper diameter) and, the 'Circularity' of interphase nuclei in root tips of 8-d-old *in vitro*-grown H2B-YFP seedlings. Scoring was performed in meristematic zone between about 15 and 70 µm above the quiescent center, excluding epidermis and the stele cells.

Supplemental References

Blilou, I., Xu, J., Wildwater, M., Willemsen, V., Paponov, I., Friml, J., Heidstra, R., Aida, M., Palme, K., and Scheres, B. (2005). The PIN auxin efflux facilitator network controls growth and patterning in Arabidopsis roots. Nature **433:** 39-44.

Cheng, Y., Cao, L., Wang, S., Li, Y., Shi, X., Liu, H., Li, L., Zhang, Z., Fowke, L.C., Wang, H., and Zhou, Y. (2013). Downregulation of multiple CDK inhibitor ICK/KRP genes upregulates the E2F pathway and increases cell proliferation, and organ and seed sizes in Arabidopsis. Plant J. **75:** 642-655.

Clough, S.J., and Bent, A.F. (1998). Floral dip: a simplified method for *Agrobacterium*-mediated transformation of *Arabidopsis thaliana*. Plant J. **16:** 735-743.

Donnelly, P.M., Bonetta, D., Tsukaya, H., Dengler, R.E., and Dengler, N.G. (1999). Cell cycling and cell enlargement in developing leaves of Arabidopsis. Dev. Biol. **215:** 407-419.

Dubin, M.J., Bowler, C., and Benvenuto, G. (2008). A modified Gateway cloning strategy for overexpressing tagged proteins in plants. Plant Methods **22:** 4:3.

Gardner, M.J., Baker, A.J., Assie, J.-M., Poethig, R.S., Haseloff, J.P. and Webb, A. A.R. (2009). *GAL4 GFP* enhancer trap lines for analysis of stomatal guard cell development and gene expression. J. Exp. Bot. ***60:*** *213-226*.

Kerschen, A., Napoli, C., Jorgensen, R., and Müller, A. (2004). Effectiveness of RNA interference in transgenic plants. FEBS Lett. **566:** 223-228.

Moulinier Anzola, J., Sieberer, T., Ortbauer, M., Butt, H., Korbei, B., Weinhofer, I., Muellner, A.E., and Luschnig C. (2010). Putative Arabidopsis Transcriptional Adaptor Protein (PROPORZ1) is required to modulate histone acetylation in response to auxin. Proc. Natl. Acad. Sci. USA **107:** 10308-10313.

Nadeau, J.A., and Sack, F.D. (2002). Control of stomatal distribution on the Arabidopsis leaf surface. Science **296:** 1697–1700.

Nakajima, K., Sena, G., Nawy, T., and Benfey, P.N. (2001). Intercellular movement of the putative transcription factor SHR in root patterning. Nature **413:** 307-311.

Nakamura, S., Mano, S., Tanaka, Y., Ohnishi, M., Nakamori, C., Araki, M., Niwa, T., Nishimura, M., Kaminaka, H., Nakagawa, T., Sato, Y., and Ishiguro, S. (2010). Gateway binary vectors with the bialaphos resistance gene, bar, as a selection marker for plant transformation. Biosci. Biotechnol. Biochem. **74:** 1315-1319.

Sabatini, S., Beis, D., Wolkenfelt, H., Murfett, J., Guilfoyle, T., Malamy, J., Benfey, P., Leyser, O., Bechtold, N., Weisbeek, P., and Scheres, B. (1999). An auxin-dependent distal organizer of pattern and polarity in the Arabidopsis root. Cell **99:** 463-72.

Sanz, L., Dewitte, W., Forzani C, Patell, F., Nieuwland, J., Wen, B., Quelhas, P., De Jager, S., Titmus, C., Campilho, A., Ren, H., Estelle, M., Wang, H., and Murray, J.A. (2011). The Arabidopsis D-type cyclin CYCD2;1 and the inhibitor ICK2/KRP2 modulate auxin-induced lateral root formation. Plant Cell **23:** 641–660.

Wen, B., Nieuwland, J., and Murray, J.A.H. (2013). The Arabidopsis CDK inhibitor ICK3/KRP5 is rate limiting for primary root growth and promotes growth through cell elongation and endoreduplication. *J. Exp. Bot.* **64:** 1135-1144.

Welch, D., Blilou, I., Immink, R., Heidstra, R. and Scheres, B. (2007). *Arabidopsis* JACKDAW and MAGPIE zinc finger proteins delimit asymmetric cell division and stabilize tissue boundaries by restricting SHORT-ROOT action. Genes Dev. **21:** 2196-2204.